WELDING RESEARCH

SUPPLEMENT TO THE *WELDING JOURNAL,* OCTOBER 2004
Sponsored by the American Welding Society and the Welding Research Council

Optimization of Shielded Metal Arc Weld Metal Composition for Charpy Toughness

Artificial neural network models can help formulate consumables

BY M. MURUGANANTH, S. S. BABU, AND S. A. DAVID

ABSTRACT. Artificial neural network models that predict the Charpy-impact toughness values as a function of composition, heat treatment, and shielded metal arc welding process parameters were coupled with multipurpose optimization software. This coupled model was used to optimize the carbon, nickel, and manganese concentrations in a weld to achieve a maximum toughness of 120 J at –60°C. The coupled model used linear and nonlinear techniques to explore the possible combinations of carbon, manganese, and nickel concentrations for a given set of welding process parameters. An optimum weld metal composition was achieved only with nonlinear methods. The number of iterations and the exploration of input parameter space varied depending upon the type of nonlinear technique. The predicted weld metal composition was in agreement with published results.

Introduction

The development of a new welding consumable for a weldment with good properties is often difficult due to complex interaction between alloying elements, welding process, process parameters, and the testing conditions. Among this wide range of variables, it is not possible to vary one variable without influencing the effect caused by the other. For example, Evans showed that, for a given shielded metal arc welding process and process parameters, increasing the titanium concentration from 7 to 30 parts per million (ppmw) led to a large increase in the toughness of Fe-C-Mn-based welds (Ref. 1). Though the concentration of titanium was varied, it influenced the effect of oxygen in the weld. In a similar manner, increasing nickel concentration in high-manganese (~2 wt-%) steel welds did not improve the toughness of the weld as would be expected otherwise. This phenomenon was explained with an increase in hardenability effect, i.e., increased nickel and manganese concentration led to the formation of martensite (Ref. 2). The above example illustrated the need for extensive trial and error experimentation guided by metallurgical principles. In the last three decades, extensive research has been done on welding consumable design and there exists a large set of experimental data relating the process, composition, and properties (Refs. 3–6). However, these welding consumable designs are not guaranteed to be the optimum, since it is not practical to explore all combinations of compositional and process variations due to the cost and time limitations.

To arrive at an optimum composition and process parameters, an alternative approach is to use computational models that have been well tested and validated with already existing experimental data. Computational models relate the input parameters (e.g., voltage, current, weld metal composition, etc.) to the output parameters (strength, toughness, microstructure, etc.). These models can be empirical, phenomenological, or integrated models (may include empirical and phenomenological models). Empirical models are either based on analytical functions or artificial neural network models that have been fitted or trained, respectively, on already existing data. The empirical models in general have limited extendibility to the range of input data used in the development stage. The phenomenological models are based on well-established principles or equations that describe particular phenomena. Many parameters used in the development of these models are derived from experimental information. The integrated models can couple many such models to relate the complex interactions between different phenomena. By interrogation of these computational models over the wide range of compositional and process parameters, it is possible to arrive at optimum composition by repeated calculations.

Optimization of welding using computational models must consider two main issues. First, the models cannot be applicable to overall input space due to its limitation on applicability. This can be solved by limiting the scope of the input data used in the calculations. Second, even with limited scope of input variables, this approach may sometimes lead to insolvability conditions, depending on the input parameters space that needs to be considered for optimization. For example, in a case where n input parameters are varied over a range of m values independently, the number of combinations that need to be evaluated by this forward modeling would amount to m^n. In a steel weld metal, if the concentrations of nickel, silicon, and manganese are allowed to vary between 0 and 10 wt-% with increments of 0.1, then the number of combinations to find the optimum will be 10^6. The 10^6 evaluations can be easily performed for a simple model that requires resources of only a small desktop computer. For example, if a model takes 0.01 s for one calculation, it will take only 2.78 h. If the model takes 8 h to run a particular case, it will take 913 years! This problem of insolvability can be removed by extending the recent advances in optimization methodologies. The current paper pertains to the evaluation of optimization software toward weld design optimization.

KEY WORDS

Consumable Design
Neural Network Modeling
Optimization Methodologies
Nonlinear Programming
Sequential Quadratic Programming
Downhill Simplex Methods
Genetic Algorithms

M. MURUGANANTH, formerly at the Metals and Ceramics Division, Oak Ridge National Laboratory, Oak Ridge Tenn., is at the School of Material Engineering, Nanyang Technological University, Singapore. S. S. BABU and S. A. DAVID are with the Metals and Ceramics Division, Oak Ridge National Laboratory.

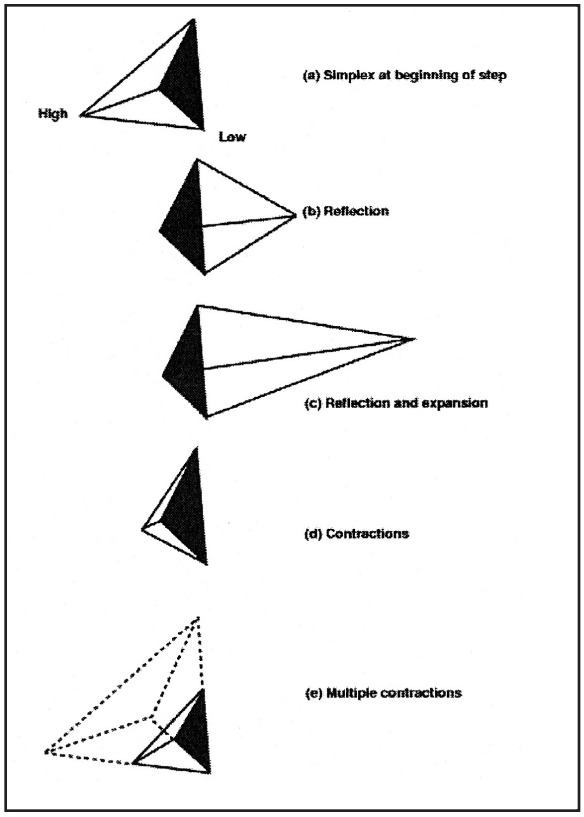

Fig. 1 — In this figure, each vertex corresponds to each dimension and the normalized value of minimum and maximum in each dimension correspond to size of these vertices. A — Simplex at the beginning of the step, here a tetrahedron. The simplex at the end of the step can be: B — a reflection away from high point (where the objective function is largest); C — a reflection and expansion away from high point; D — a contraction along one dimension from the high point; E — a contraction along all dimensions toward the low point. An appropriate sequence of such steps will always converge to a minimum of the objective function (Ref. 9).

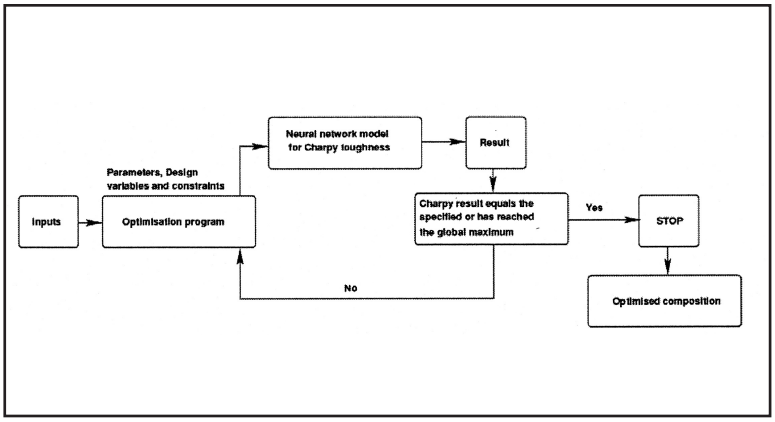

Fig. 2 — Flowchart showing the optimization procedure.

Optimization Methodologies

Optimization techniques can be broadly classified under linear and nonlinear programming methods. The linear programming methods can be used to determine the optimum when the variables are linearly related to the objective function and the constraints. An example is the relation between *c*/*a* ratio in a body-centered tetragonal structure of martensite and carbon concentration. But such ideal relations do not exist in the relation between alloying elements and mechanical properties. Under such complex relations between input and output parameters, the nonlinear programming methods, including sequential quadratic programming (SQP), downhill simplex methods, and genetic algorithms are commonly used (Ref. 7). Some of these nonlinear methods are briefly explained below.

In SQP, the objective function assumes a quadratic relationship with the variables (design) and parameters. Sequential quadratic programming can be used for both constrained and unconstrained optimization problems. A constrained optimization involves specification of constraints. In SQP, search for an optimum is made by finding a solution to a quadratic subproblem at each iteration. This method is used for problems with a smooth objective function.

Downhill simplex methods can be illustrated based on a geometric figure in N dimensions, consisting of $N + 1$ points (or vertices) and all their interconnecting line segments, polygonal faces, etc. Here, the notation N corresponds to the number of dimensions, which is related to the number of input parameters. In two dimensions, a simplex is a triangle. In three dimensions, it is a tetrahedron — not necessarily a regular tetrahedron. The downhill simplex method takes a series of steps, most steps just moving the point of the simplex where the objective function is largest through the opposite face of the simplex to a lower point (where the objective function becomes the minimum). These steps are called reflections, and they are constructed to conserve the volume of the simplex. The method also expands the simplex in one or another direction to take larger steps to expedite the speed of convergence. Conversely, the method also shrinks the simplex in all directions, allowing it to settle in a minimum. These are called contractions. This method is said to have the highest proba-

Table 1 — Input Variables Used to Train the Models for Establishing a Network of Composition, Heat Treatment, and Welding Parameters with Toughness (PWHT is Postweld Heat Treatment) (All elements in wt-% unless otherwise specified)

Input Variables	Minimum	Maximum	Mean	Std. Dev.
Carbon	0.02	0.19	0.07	0.021
Silicon	0.01	1.63	0.4	0.13
Manganese	0.23	2.31	1.2	0.42
Sulphur	0.002	0.14	0.0078	0.008
Phosphorus	0.003	0.25	0.01	0.014
Nickel	0	9.4	0.6	1.6
Chromium	0	11.78	0.5	1.4
Molybdenum	0	1.54	0.2	0.34
Vanadium	0	0.53	0.01	0.045
Copper	0	2.18	0.06	0.22
Cobalt	0	0.016	0.0007	0.0027
Tungsten	0	3.8	0.008	0.2
Oxygen (ppmw)	63	1535	406.2	112.3
Titanium (ppmw)	0	770	100.03	135.4
Nitrogen (ppmw)	21	1000	98.3	67.8
Boron (ppmw)	0	200	13.8	34.3
Niobium	0	1770	39.3	136.8
Heat input (kJ mm^{-1})	0.6	6.6	1.19	0.7
Interpass temperature (°C)	20	350	200.19	31.23
PWHT temperature (°C)	20	760	185.36	257.24
PWHT time (h)	0	100	2.7	6.13
Test temperature (°C)	–196	136	–44.25	36.13

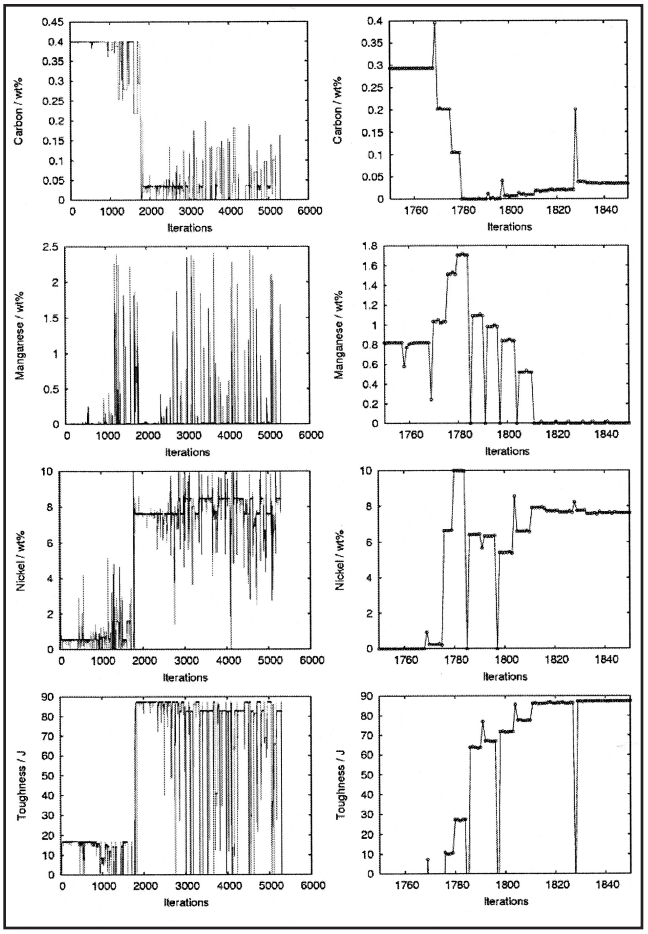

Fig. 3 — The sequential quadratic programming method succeeds in finding the optimum. Plots on right column are presented for clarity, focusing the region where the optimum was first found.

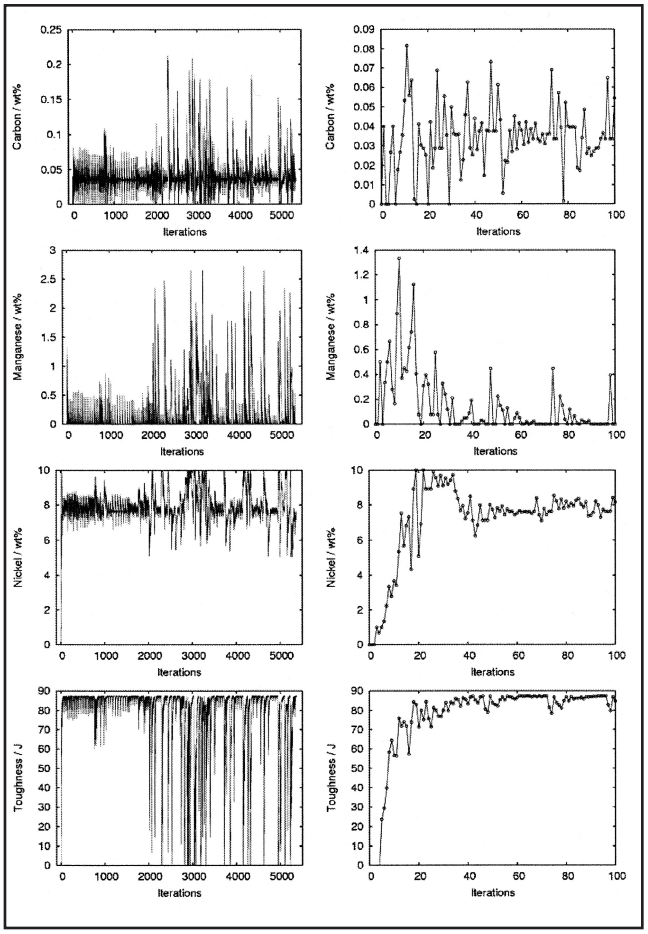

Fig. 4 — Downhill simplex finds the optimum in only 67 iterations, unlike any of the other methods. Plots on right column are presented for clarity, focusing the region where the optimum was first found.

bility of finding the global minimum when it is started with initial big steps (Ref. 8). Figure 1 shows reflections, contractions, and expansions in a clear manner (Refs. 7–9).

Genetic algorithms use mutation or recombination and selection to minimize the objective function. In this algorithm, a point is chosen in the design space, and a lot of points are generated around this point. This process is called mutation. Now, the best of all the points is selected. In recombination, a random number of points exchange values. Recombination and mutation are used in such a way so as to allow points to move toward a direction of objective function minimization. Genetic algorithms converge rapidly, but have trouble converging to the exact solution (Ref. 7).

A hybrid or local optimizer uses either of the above-described optimizers in an alternating manner, according to the need. For example, to converge fast toward the global minimum, the downhill simplex method may be used as a start, but when it comes to dealing with complex topographies, genetic optimizers do the

Table 2 — Parameters and Design Variables Used at the Start of Optimization

Element	Base value	Minimum	Maximum
Carbon (wt-%)	0.0	0	0.4
Silicon (wt-%)	0.65	—	—
Manganese (wt-%)	0.0	0	5
Sulphur (wt-%)	0.006	—	—
Phosphorus (wt-%)	0.013	—	—
Nickel (wt-%)	0.0	0	10
Chromium (wt-%)	0.21	—	—
Molybdenum (wt-%)	0.4	—	—
Vanadium (wt-%)	0.011	—	—
Copper (wt-%)	0.03	—	—
Cobalt (wt-%)	0.009	—	—
Tungsten (wt-%)	0.005	—	—
Oxygen (ppmw)	380	—	—
Titanium (ppmw)	80	—	—
Nitrogen (ppmw)	180	—	—
Boron (ppmw)	1	—	—
Niobium (ppmw)	10	—	—
Heat input (kJ mm^{-1})	1	—	—
Interpass temperature (°C)	250	—	—
PWHT temperature (°C)	250	—	—
PWHT time (h)	16	—	—
Test temperature (°C)	–60	—	—

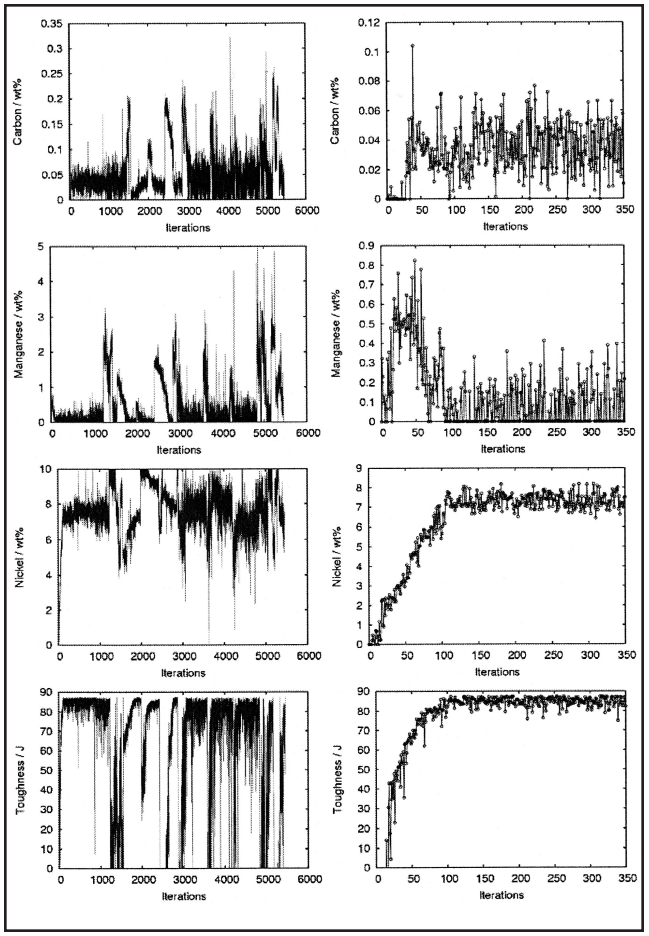

Fig. 5 — Genetic optimizers found the optimum after 323 iterations. Plots on right column are presented for clarity, focusing the region where the optimum was first found.

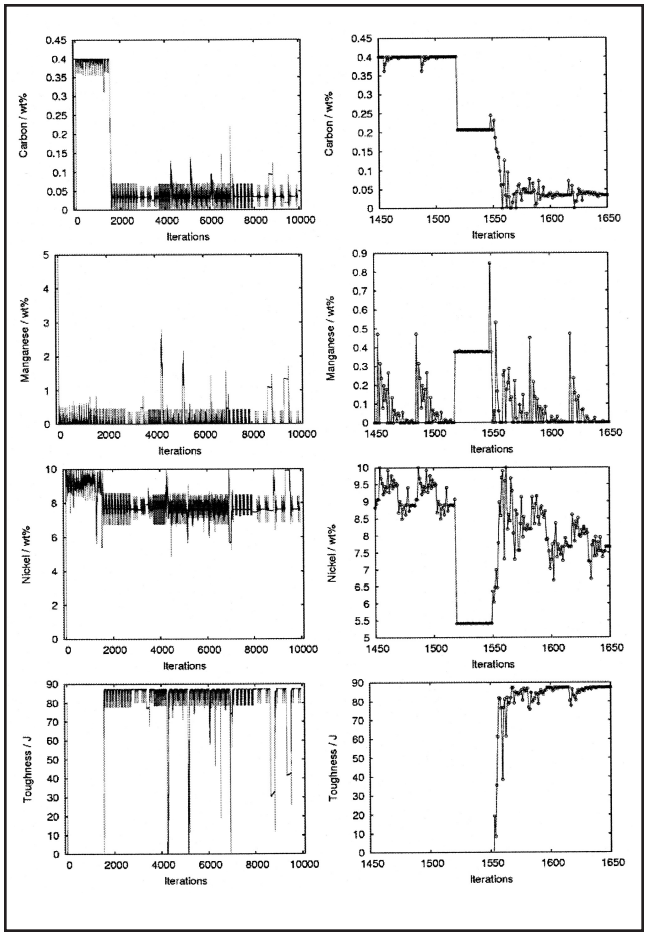

Fig. 6 — Hybrid optimizers succeeded in finding the optimum after 1600 iterations. Plots on right column are presented for clarity, focusing the region where the optimum was first found.

best. Hence, such an alternative implementation of optimizers is chosen by the pointer technology used in the hybrid/local optimizers. How this randomness is chosen by the local/hybrid optimizer is not presented here, due to proprietary reasons.

In this paper, we evaluated the above optimization methodologies to arrive at optimum weld composition by coupling an optimization software with a neural network model that relates the composition, welding process parameters, heat treatment, and Charpy toughness.

Optimization Calculations

The first step in the optimization for weld deposit composition is the selection of a computer model that relates the composition, welding process parameters, heat treatment, and Charpy toughness. In this research, we adopted a recently developed artificial neural network (ANN) model for Charpy toughness of steel welds (Refs. 2, 10). Artificial neural networking is an empirical modeling technique. It uses nonlinear regression in combination with a probabilistic approach to create a network between input variables and the output variable. Applicability of these models for prediction is mainly governed by the region covered by the input data on which they are trained, and the scatter in data. Within the regions covered by the input variables during training, the accuracy of the prediction becomes higher. A model was developed using this technique on a dataset consisting of 4000 data lines comprising composition, welding process parameters, Charpy test temperature, and preweld and postweld heat treatments. The range of the input variables gives an approximate representation of the model applicability (Table 1). It is important to note that welding process parameters are lumped into one parameter, i.e., heat input in this model. For information about the scatter in data, readers are referred to Ref. 2 *(http://www.msm.cam.ac.uk/phase-trans/2002/ananth.thesis.pdf)* and Ref. 10. The data used in the neural net simulation contain a wide range of elemental concentrations and are significant even with nickel concentrations in the range of 6 to 10 wt-%. The benefits of using the Bayesian neural network used in this paper are also discussed in Ref. 10. It is important to note that this ANN model is also capable of describing the uncertainty in the predictions.

In the second step, the above-mentioned ANN model was coupled with a commercial software package, *Epogy* (by Synaps Inc.), which is capable of performing both linear and nonlinear optimization (Ref. 7). This module was developed and evaluated on a Redhat Linux v9.0 computer. The steps involved in the calculations are schematically illustrated in Fig. 2. At the start of optimization, an initial set of input variables is chosen by the user. Moreover, the variables that need to be varied (defined as design variables) and the variables that have to be kept constant (defined as parameters) are identified. The optimizer then interrogates the ANN model to evaluate the toughness for the initial set of input data. Then, the difference between the target

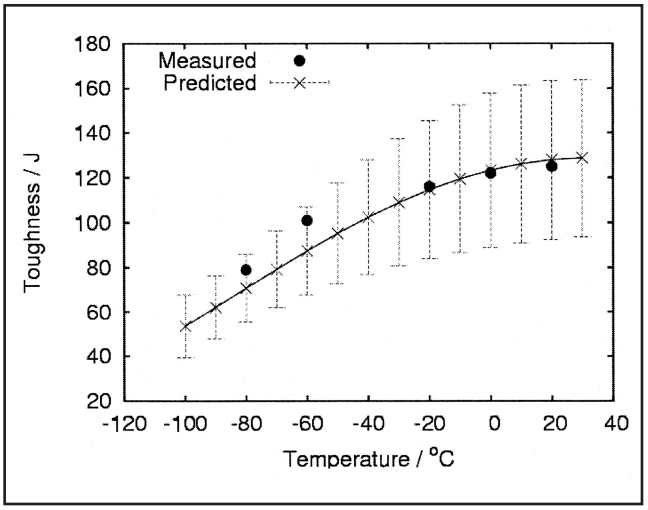

Fig. 7 — Comparison of Charpy toughness predicted using artificial neural network models and measured Charpy toughness values.

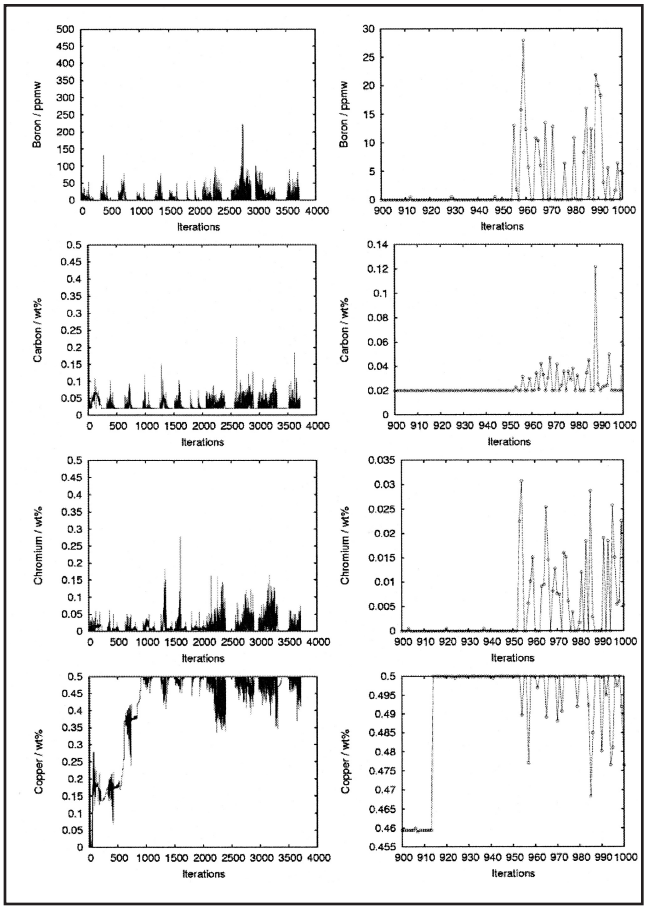

Fig. 8 — Plots showing the exploration done by local/hybrid optimizer for B, C, Cr, and Cu.

and the current calculation is evaluated for meeting the required criteria. On not meeting the criteria, the optimizer algorithm decides the direction in which the design variables need to be varied. Subsequently the whole process is repeated. On meeting the criteria, the module stops the optimization. If, after a large number of iterations, there is no improvement in the calculated value, then the module reports the highest possible toughness attainable for the given set of design variables and constraints.

In the first set of evaluations (Test A), the optimization techniques were tested for finding an optimum composition by considering nickel, manganese, and carbon concentrations as design variables. The constant parameter values are shown in Table 2. These parameters were selected based on earlier experimental research performed on similar welds (Refs. 2, 10). Therefore, Test A is aimed at evaluating the robustness of different optimization techniques. In the second set of evaluations (Test B), the design variables were increased from 3 to 13. The design variables included B, C, Cr, Cu, Mn, Mo, N, Nb, Ni, Si, Ti, V, and W. The criterion for optimization was set as attaining a Charpy toughness of 120 and 200 J at –60°C for Test A and Test B, respectively.

Results

Linear programming methods (described under the heading "Optimization Methodologies") failed to find an optimum in Charpy toughness. The linear methods increased the carbon and nickel concentrations but did not explore any other regions of input space. Hence, there was no possibility of finding the optimum using this method. This supports the earlier notion that Charpy toughness is not related to the input variables in a linear fashion.

The next four paragraphs present the results obtained from nonlinear optimization techniques. Figures 3–6 associated with these discussions are presented in a two-column format. Figures on the left column give an idea about the trend that each optimizer under consideration followed throughout the optimization run. Figures on the right column focus the iterations when the optimizer first reached the optimum value.

In the first part of the simulation, the SQP method increased the carbon concentration to ~0.4 wt-% (see Fig. 3) and explored the manganese and nickel concentration variations. In the next part, the carbon content was reduced to ~0.05 wt-% and the nickel concentrations were increased above 6 wt-%. The result shows that the SQP method clearly identified that the maximum rate of increase in toughness would be achieved by an increase in nickel content. Immediately after this step, around 1836 iterations, the SQP method reached the optimum composition for the first time. Interestingly, the SQP method explored only until 2.5 wt-% Mn, whereas the region of input space defined for manganese was from 0 to 5 wt-%. With further iterations, carbon, nickel, and manganese concentrations oscillated around this optimum composition before the termination of the optimization exercise.

Downhill simplex methods adapted a different strategy by varying carbon, manganese, and nickel concentrations simultaneously. Carbon was varied between 0 and 0.06 wt-%, manganese between 0 and 0.5 wt-%, and nickel between 6.2 and 8.3 wt-% — Fig. 4. The plots also show that the downhill simplex method identified the importance of increasing the nickel concentration within 20 iterations. Similarly, the importance of reducing the Mn levels to very low levels was also identified. The optimum composition was reached in 67 iterations for the first time. With further iterations until 5000, the downhill simplex method explored variations of carbon and manganese. Nevertheless, the downhill simplex method explored only until 0.2 wt-% for carbon and 2.7 wt-% for manganese, and did not explore near the maximum value specified in the design variable range.

Genetic optimizers adapted a step-by-step process in which, during the first 200 iterations, carbon concentration was kept at 0 wt-%, while nickel was increased gradually by varying manganese concentrations — Fig. 5. After a certain concentration of nickel, the carbon contents were also increased. The optimum composition was reached in 323 iterations for the first time. It is interesting to note that the shape of

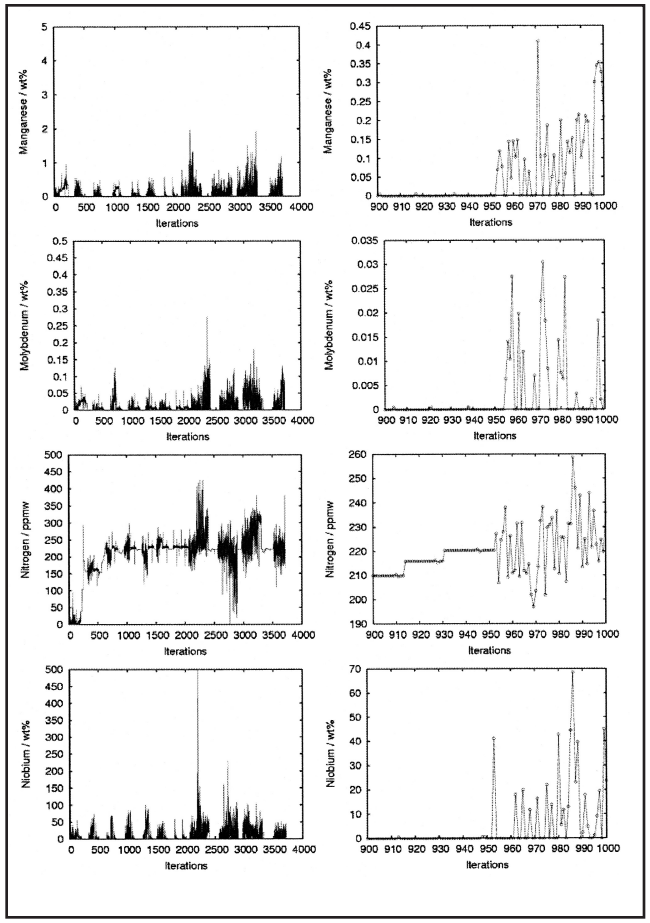

Fig. 9 — Plots showing the exploration done by local/hybrid optimizer for Mn, Mo, N, and Nb.

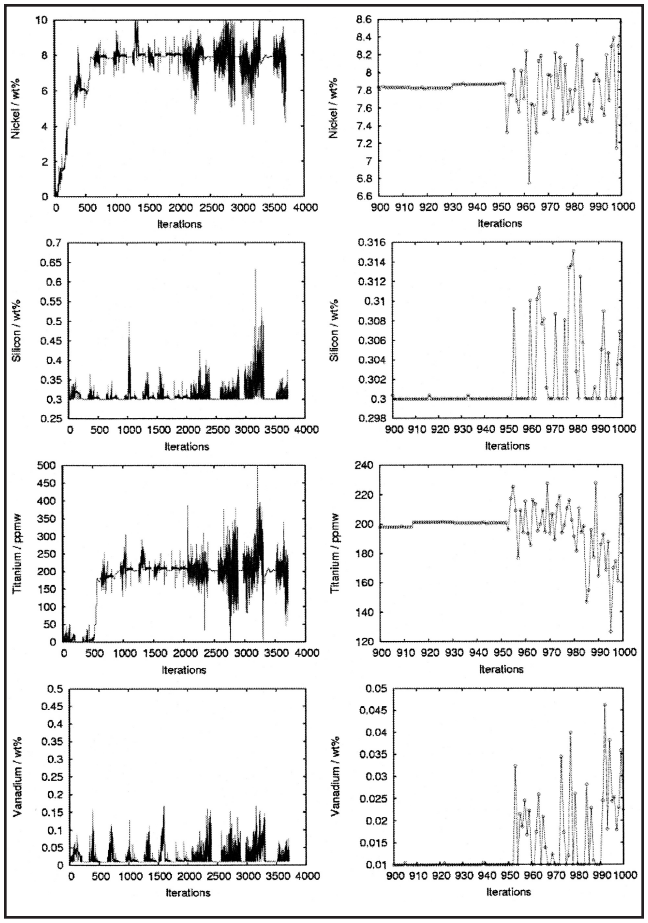

Fig. 10 — Plots showing the exploration done by local/hybrid optimizer for Ni, Si, Ti, and V.

variation of manganese and nickel concentration with the number of iterations before reaching the optimum value appears similar to that of the downhill simplex method. In other words, initially the manganese and nickel were increased, and then the manganese was reduced while increasing the nickel content. The only difference is that the genetic algorithm was slower in reaching the higher nickel and lower manganese concentrations that are closer to the optimum level. After reaching the optimum composition, the genetic optimizer explored the major part of the input space. This is in contrast to previous methods. Similar to other methods, the genetic optimizers did not explore very high carbon concentrations.

The next set of calculations considered an optimizer based on the local or hybrid methodology, and the results are shown in Fig. 6. It is interesting to note that in this methodology, the first part of optimization led to increased carbon concentration close to 0.4 wt-%, the maximum value defined in the input range, during the first 1500 iterations. Subsequently, the optimizer briefly reduced the carbon to 0.2 wt-% and explored at higher manganese and lower nickel contents. At this stage, the optimizer reached a plateau with no improved prediction of toughness. With further iterations, in the third part of the calculations, the optimizer correctly found the importance of reducing the carbon to the next level in the range of 0.05 wt-%. At this stage, the optimum composition was reached with increased nickel concentration after 1600 iterations. Although, the hybrid optimizer was slow, the methodology explored all of the input regions defined for all the three variables. This allows for testing the hypothesis that the final optimized composition (presented in the next paragraph) is the global optimum.

The performances of all optimization methods in Test A are compared in Table 3. It is reassuring to note that all the optimizers gave one optimized composition after the completion of Test A. However, the predicted toughness for this optimum composition was 87 ± 20 J. Therefore, the optimized value did not meet the required criteria of 120 J at –60°C. Nevertheless, the optimum composition was used to predict the variation of toughness with temperature using the ANN model. The optimization for the three variables C, Mn, and Ni compared well with that of the experimental results (Ref. 2). The experimental optimum weld composition was Fe -0.025 C -0.65 Mn -6.6 Ni -0.65 Si -0.038 O -0.018 N -0.013 P -0.006 S -0.03 Cu -0.008 Ti (wt-%) and the corresponding measured toughness of 101 J at –60°C is very similar to the predicted optimum weld composition. The predicted optimum weld composition was further compared with experimental measurements by predicting the variation of toughness with temperature — Fig. 7. The comparison shows fair agreement with the currently attained optimum composition and proves the power of this coupled ANN-optimization model.

In Test B, the effect of considering a wide range of design variables was explored with a hybrid optimizer. The optimum composition was arrived after 930 iterations (see Figs. 8–11). Figures 8–11 illustrate the trend with which the hybrid optimizer varied alloying elements. In Table 4, Test B gives the optimum composition obtained in this analysis. It can be seen that the optimizer has reduced Mn, Cr, Mo, W, B, and Nb to zero — on the

other hand, increasing the contents of Ti and N to very high levels of 202.5 and 222.4 ppmw, respectively. However, there are no experimental data with such high levels of Ti, N, and Ni. Possible reasons for selection of this weld composition will be discussed in the next section.

Discussion

In the three-variable optimization case, downhill simplex and genetic optimizers follow a trend that can be interpreted using metallurgical principles, unlike SQP and hybrid optimizers.

Before reaching the optimum composition after 67 iterations with downhill simplex, there is a slow increase in carbon and manganese concentrations at lower nickel contents. Increase in carbon and manganese concentration improves the toughness by increasing the amount of acicular ferrite in the microstructure. However, as the concentration of nickel is raised above 7 wt-%, the hardenability is high enough to result in a martensitic microstructure (Ref. 2). Hence, above this critical concentration of nickel, any increase in manganese or carbon concentration leads to an even harder martensite, thus reducing toughness; whereas a nickel martensite at low carbon contents is expected to be tougher (Refs. 2, 10). Thus, the optimum composition has low carbon and zero manganese with high nickel concentration.

Due to innate characteristics like reflection and contraction, the downhill simplex methods have explored regions even at higher nickel contents (near the defined maximum value minus 10 wt-%) than the optimum nickel concentration; whereas genetic optimizers have gradually increased the nickel concentration to the optimum level, after which they have not explored. This can be attributed to the restrictions imposed on the step sizes, which are relatively smaller and constant in genetic methods compared to the downhill simplex methods (Ref. 7).

All the optimizers arrived at the same optimum composition in the case studied in Test A. Thus, it is appropriate to consider this composition as the global optimum. Under this specific case, downhill

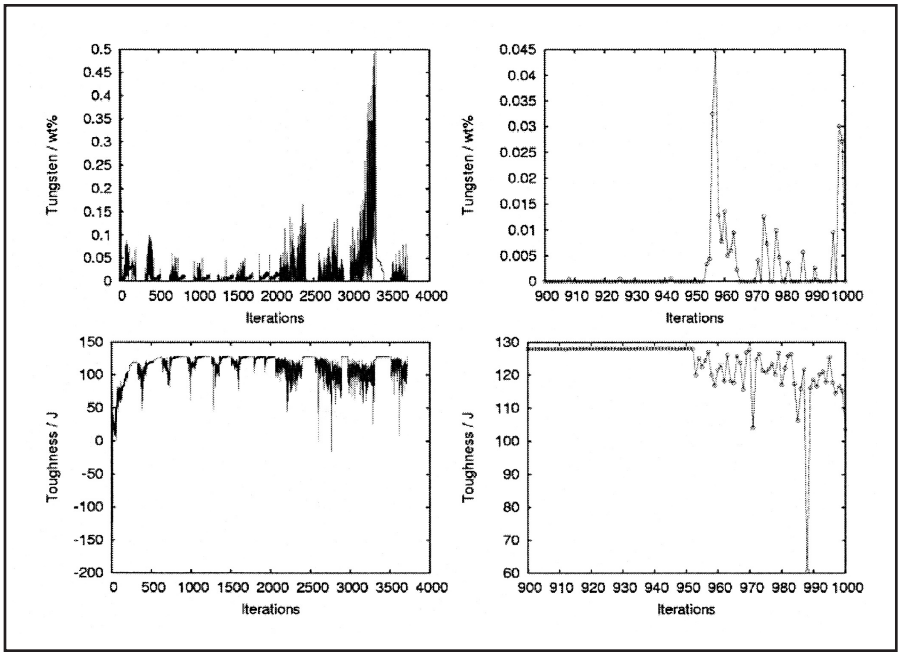

Fig. 11 — Plots showing the exploration done by local/hybrid optimizer for W. Also shown is the corresponding toughness at each iteration, where the alloying elements were varied.

Table 3 — Comparison of Different Optimizers in Test A, for Successfully Finding Optimum Composition and the Number of Iterations Made before Finding the Optimum (The region of input space explored by the optimizer is also presented. Note that while comparing the performance of each optimizer based on the number of iterations, the starting point for all the optimization runs need to be the same)

Optimizer	Success or failure	Number of iterations before arriving at optimum	Region of input space explored by the optimizer looking for an optimum (This decides the chance for getting into a local optimum)	Optimized values (wt-%)
Linear	Failed	—	—	
SQP	Success	1836	C (0–0.4) Mn (0–2.46) Ni (0–10)	0.034 0 7.6
Downhill simplex	Success	67	C (0–0.2) Mn (0–2.72) Ni (0–10)	0.034 0 7.6
Genetic	Success	323	C (0–0.32) Mn (0–5) Ni (0–10)	0.034 0 7.6
Local/hybrid	Success	1600	C (0–0.4) Mn (0–5) Ni (0–10)	0.034 0 7.6

Table 4 — Parameters and Design Variables Used at the Start of Optimization

Element	Base value	Minimum	Maximum
Carbon (wt-%)	0.0	0.02	0.5
Silicon (wt-%)	0.0	0.3	0.7
Manganese (wt-%)	0.0	0.0	5
Sulphur (wt-%)	0.006	—	—
Phosphorus (wt-%)	0.013	—	—
Nickel (wt-%)	0.0	0.0	10
Chromium (wt-%)	0.0	0.0	0.5
Molybdenum (wt-%)	0.4	0.0	0.5
Vanadium (wt-%)	0.0	0.01	0.5
Copper (wt-%)	0.0	0.0	0.5
Cobalt (wt-%)	0.009	—	—
Tungsten (wt-%)	0.0	0.0	0.5
Oxygen (ppmw)	380	—	—
Titanium (ppmw)	0.0	0.0	500
Nitrogen (ppmw)	0.0	0.0	500
Boron (ppmw)	0.0	0.0	500
Niobium (ppmw)	0.0	0.0	500
Heat input (kJ mm^{-1})	1	—	—
Interpass temperature (°C)	250	—	—
PWHT temperature (°C)	250	—	—
PWHT time (h)	16	—	—
Test temperature (°C)	–60	—	—

simplex can be ranked the best as it arrived at the global optimum in only 67 iterations.

As already discussed in the previous section, since the use of individual optimizers did not cover all of the input space (Test B), the hybrid optimizer was used in optimizing 13 variables. The hybrid optimizers first reached the optimum after 1600 iterations for a three-variable case. With the increase in the number of design variables, it is expected that the number of iterations to arrive at the optimum would also increase. Whereas, in the present case where 13 variables were optimized, the hybrid optimizer reached the optimum in only 930 iterations as compared to 1600 iterations for the three-variable case. This is due to the randomness involved in the hybrid optimizer in selecting a particular optimization algorithm for a given kind of problem (Ref. 7).

The level of uncertainty predicted by ANN in Test A was 20 J and in Test B was 70 J. As mentioned earlier, the uncertainty is related to the training data used by the ANN model developed and is predicted using the methodology described in Refs. 2 and 10. Careful analyses showed that the input data do not contain any weld compositions with very low carbon (<0.02 wt-%) and very high titanium (>120 ppmw) and high nitrogen (>190 ppmw). It is important to note that the optimum composition in Test B contains 0.02 wt-% carbon, 202 ppmw titanium, and 222 ppmw nitrogen. Since this prediction is beyond the scope of the training data, one would expect a high uncertainty in the ANN model predictions. In agreement, the ANN model correctly predicted that the uncertainty in the calculated toughness was 70 J. In contrast, the optimum composition predicted by Test A was within the scope of the input space of the ANN model; as a result, the ANN model predicted a lower uncertainty of toughness prediction: 20 J.

Further, the optimization analysis resulted in a zero concentration of Mn, Cr, Mo, W, B, and Nb; whereas C, V, and Si assumed the minimum concentration in the allowed concentration range, unlike Cu, whose concentration was raised to the maximum with Ni, Ti, and N assuming an optimized value. From toughness point of view, it is very sensible that elements like C, Mn, Cr, and B that increase the hardenability should be kept at low concentrations. Raiter et al. have analyzed the effect of molybdenum on carbon manganese steels and have concluded that molybdenum decreases the ductile-brittle transition temperature (Ref. 12). However, this need not be true in the case of higher nickel welds. In the microstructure of carbon-manganese welds that consists of acicular ferrite, molybdenum is known to increase acicular ferrite microstructure in the reheated regions leading to an increase in the toughness (Ref. 12). Molybdenum also increases the hardenability of the alloy. But there is no account in literature about the molybdenum effect on welds containing martensite, as is the case with high-nickel welds.

Similarly, titanium increases the amount of acicular ferrite in carbon-manganese steels, thus improving the toughness (Refs. 1, 3–5). Higher titanium contents in combination with higher nickel levels cannot have the same effect in titanium on formation of acicular ferrite. Instead, it should have some complicated role in improving the toughness of a martensitic microstructure.

Increased silicon concentration may affect the inclusion content and microstructure evolution in a complex way. Evans (Ref. 13) has shown that silicon addition may decrease the oxygen pickup in the weld and also may increase the acicular ferrite at low levels of manganese concentrations, and may not have any significant effect at high manganese concentrations. Cr, W, Nb, and V are carbo-nitride formers that decrease the toughness because of precipitation of undesirable precipitates and solid-solution hardening. Also, these elements increase the hardenability of the steel weld drastically.

High nitrogen concentrations can cause porosity and are deleterious to toughness (Ref. 1). Evans has concluded that nitrogen has a varying effect on the toughness of C-Mn welds, depending on the concentration of Ti and B (Ref. 1). It was shown that high nitrogen contents decrease toughness in the presence of high titanium concentrations (>250 ppmw) (Ref. 1). But the same effect of nitrogen may not hold appropriate for the high-nickel welds.

As the optimized composition has a high concentration of nickel and nitrogen, the microstructure is speculated to be martensitic along with some amount of retained austenite at the cooling rates involved in welding.

From the research point of view, it would be really interesting to make an experimental weld of the optimized composition specified in Test B. The weld metal may, however, have poor strength, as most of the solid-solution hardening elements are set to zero.

The above discussion leads to an important question: Is it possible to optimize for both strength and toughness? Therefore, some preliminary research was done to optimize for both strength and toughness by coupling the ANN model for toughness, the ANN model for room-temperature yield strength (Ref. 2), and the optimization software (Ref. 14). In this hypothetical research, the objective was to maximize the yield strength to 1000 MPa $\left(YS^{RT}_{current}\right)$ at room temperature and the Charpy toughness of 90 J $\left(CVN^{-60^{\circ}C}_{current}\right)$ at –60°C. For this analysis, an objective function has to be defined as a target for the optimization software and it is set to minimize the difference between predicted

and target values (LSE) for both Charpy toughness and yield strength, which follows.

$$LSE = \left(\frac{CVN_{current}^{-60^{\circ}C} - 90}{90} \right)^2 + \left(\frac{YS_{current}^{RT} - 1000}{1000} \right)^2 = 0 \qquad (1)$$

The hybrid optimizer was used for both optimizations. Six input parameters, i.e., carbon, manganese, nickel, copper, titanium, and interpass temperatures, were varied by the optimizer to look for the optimum composition that satisfied Equation 1, while all other parameters were kept constant (Table 2). The optimizer arrived at an optimum composition after 136 iterations. The optimum parameters were predicted to be 0.032 wt-% C, 0.0 wt-% Mn, 9.38 wt-% Ni, 0.086 wt-% Cu, 60 ppmw Ti, and an interpass temperature of 210°C, while the base composition of the weld metal was Fe–0.65Si–0.0Mn –0.006Cu–0.038O–0.018N–0.013P–0.00S (wt-%). For this condition, the predicted Charpy value was 80 ± 20 J at –60°C and the predicted room-temperature yield strength was 866 ± 89 MPa. It is noteworthy that this analysis showed that it is not possible to achieve 1000 MPa yield strength while maintaining a toughness of 90 J, and the predicted compromise was 866 MPa yield strength at room temperature and 80 J Charpy toughness value at –60°C. In addition, to achieve this result, the optimizer also increased the interpass temperature to 210°C. In the same analyses, relaxation of input ranges above the trained limits given in Table 1 led to reduction of carbon to 0.01 wt-%, increase of nickel to 10 wt-%, reduction of copper to 0.006 wt-%, reduction of titanium to 32 ppmw, and an increase in the interpass temperature to 300°C. However, the predicted toughness of 86 ± 18 J at –60 °C and predicted room-temperature yield strength of 840 ± 105 MPa are not significantly different from the earlier predictions. This analysis also showed that the selection of objective function and the number of input parameters, and the range of input parameters that can be varied during optimization, have a significant effect on the optimization results. The optimum composition predicted by this coupled strength and toughness optimization has not yet been validated by experiment and is the focus of the ongoing research.

Table 5 — Optimized Composition and the Maximum Obtainable Charpy Toughness for the Given Base Composition and Process Parameters as Suggested by All the Optimizers (Test A for three variable optimization involving C, Mn, and Ni. Test B pertains to the 13-variable optimization)

Element	Test A	Test B
Carbon (wt-%)	0.034	0.02
Silicon (wt-%)	0.65	0.3
Manganese (wt-%)	0.0	0.0
Sulphur (wt-%)	0.006	0.006
Phosphorus (wt-%)	0.013	0.013
Nickel (wt-%)	7.6	7.9
Chromium (wt-%)	0.21	0.0
Molybdenum (wt-%)	0.4	0.0
Vanadium (wt-%)	0.011	0.009
Copper (wt-%)	0.03	0.5
Cobalt (wt-%)	0.009	0.0089
Tungsten (wt-%)	0.005	0.0
Oxygen (ppmw)	380	380
Titanium (ppmw)	80	202.5
Nitrogen (ppmw)	180	222.4
Boron (ppmw)	1	0.0
Niobium (ppmw)	10	0.0
Heat input (kJ mm^{-1})	1	1
Interpass temperature (°C)	250	250
PWHT temperature (°C)	250	250
PWHT time (h)	16	16
Test temperature (°C)	–60	–60
Maximum toughness obtainable (J)	87	128
Uncertainty	20	70

Conclusions

An artificial neural network model was coupled with optimization software to predict weld metal composition that will maximize the toughness at –60°C. The coupled model used linear and nonlinear techniques to explore possible combinations of carbon, manganese, and nickel concentrations for a given set of welding process parameters. The analysis was performed with different optimization techniques, including simple linear and nonlinear sequential quadratic programming (SQP), downhill simplex, genetic algorithm, and local/hybrid methodology. The downhill simplex method arrived at optimum composition with the minimum number of iterations; however, it did not explore the full scope of input parameters space. In contrast, the local/hybrid method arrived at optimum composition after 1600 iterations; however, it did explore the full scope of input parameters space.

The predicted weld metal composition was Fe–0.034C–0Mn–7.6Ni–0.65Si –0.038O–0.018N–0.013P–0.006S (wt-%) and toughness at –60°C was 87 J ± 20 J. The published toughness for this weld was 101 J. This shows the applicability of coupled optimization and forward models to design weld metal composition.

Another interesting analysis done for optimizing 13 different variables proved that the optimum was not the same as in the case where C, Ni, and Mn were varied. Preliminary work with coupled optimization of strength and toughness led to a weld metal composition with high (>10 wt-%) nickel concentration. Both these predictions have not been experimentally verified, though.

Acknowledgments

The optimization process module development presented in this paper is based on research sponsored by the Division of Materials Science and Engineering (SSB and SAD), and the application of the hybrid module toward composition optimization is based on research sponsored by the Office of Energy Efficiency and Renewable Energy, Office of Industrial Technologies Program, Supporting Industries Activity (MM and SSB), U.S. Dept. of Energy, under contract DE-AC05-00OR22725 with UT-Battelle, LLC. The authors would further like to acknowledge David Kokan and team, Epogy Inc., for their valuable discussions.

References

1. Evans, G. M. 1993. The effect of titanium in manganese-containing SMA weld deposits. *Welding Journal* 72(3): 123-s to 133-s.

2. Murugananth, M. 2002. Design of welding alloys for creep and toughness. Ph.D. thesis, University of Cambridge, U.K.

3. Evans, G. M. 1997. Effect of aluminum and nitrogen on Ti-B containing steel welds. *Welding Journal* 76(10): 431-s to 441-s.

4. Evans, G. M. 1995. Microstructure and properties of ferritic steel welds containing Al and Ti. *Welding Journal* 74(8): 249-s to 261-s.

5. Evans, G. M. 1998. Effect of nitrogen on C-Mn steel welds containing titanium and boron. *Welding Journal* 77(6): 239-s to 248-s.

6. Evans, G. M. 1996. Microstructure and

properties of ferritic steel welds containing Ti and B. *Welding Journal* 75(8): 251-s to 260-s.

7. Synaps Inc. *Epogy 2003 User's Guide.*

8. Nelder, J. A., and Mead, R. 1965. Downhill simplex method in multidimensions. *Computer Journal* 7:308–313.

9. William, H. P., Saul, T. A., William, T. V., and Brian, F. P. *Numerical Recipes in C: The Art of Scientific Computing.* Second ed. Cambridge University Press.

10. Murugananth, M., Bhadeshia, H. K. D. H., Keehan, E., Andrén, H. O., and Karlsson, L. 2002. Strong and tough steel welds. Eds. H. Cerjak and H. K. D. H. Bhadeshia. *Mathematical Modelling of Weld Phenomena VI.* Institute of Materials. pp. 205–229.

12. Van der Velden, A., and David, K. 2002. The synaps pointer optimization engine. *Proceedings of DETC/CIE: Computers and Information in Engineering Conference.* Sept. 29–Oct. 2, Montreal.

13. Raiter, V., and Gonzalez, J. C. 1989. Influence of molybdenum on the microstructure and properties of weld metal with different manganese contents. *Canadian Metallurgical Quarterly* 28(2): 179–185.

14. Evans, G. M., and Bailey, N. 1997. *Metallurgy of Basic Weld Metal.* Cambridge, U.K.: Abington Publishing.

15. Murugananth, M., Babu, S. S., and David, S. A. 2004. Unpublished research. Oak Ridge National Laboratory.

WELDING JOURNAL

Instructions and Suggestions for Preparation of Articles

Text

- approximately 1500–3500 words in length
- submit hard copy
- submissions via disk or electronic transmission — preferred format is Mac but common PC files are also acceptable
- acceptable disks include floppy, zip, and CD.

Format

- include a title
- include a subtitle or "blurb" highlighting major point or idea
- include all author names, titles, affiliations, geographic locations
- separate paper into sections with headings

Photos/Illustrations/Figures

- glossy prints, slides, or transparencies are acceptable
- black and white and color photos must be scanned at a minimum of 300 dpi
- line art should be scanned at 1000 dpi
- photos must include a description of action/object/person and relevance for use as a caption
- prints must be a minimum size of 4 in. x 6 in., making certain the photo is sharp
- do not embed the figures or photos in the text
- acceptable electronic format for photos and figures are EPS, JPEG, and TIFF. TIFF format is preferred.

Other

- illustrations should accompany article
- drawings, tables, and graphs should be legible for reproduction and labeled with captions
- references/bibliography should be included at the end of the article

Editorial Deadline

- January issue deadline is November 11
- February issue deadline is December 10
- March issue deadline is January 13
- April issue deadline is February 10
- May issue deadline is March 10
- June issue deadline is April 9
- July issue deadline is May 12
- August issue deadline is June 13
- September issue deadline is July 11
- October issue deadline is August 11
- November issue deadline is September 12
- December issue deadline is October 10

Suggested topics for articles

- case studies, specific projects
- new procedures, "how to"
- applied technology

Mail to:

Andrew Cullison
Editor, Welding Journal
550 NW LeJeune Road
Miami, FL 33126
(305) 443-9353, x 249; FAX (305) 443-7404
cullison@aws.org